



HAL
open science

Peptidomic analysis of the host-defense peptides in skin secretions of the Amazon river frog *Lithobates palmipes* (Ranidae)

Milena Mechkarska, Gervonne Barran, Jolanta Kolodziejek, Laurent Coquet, Jérôme Leprince, Thierry Jouenne, Norbert Nowotny, J. Michael Conlon

► To cite this version:

Milena Mechkarska, Gervonne Barran, Jolanta Kolodziejek, Laurent Coquet, Jérôme Leprince, et al.. Peptidomic analysis of the host-defense peptides in skin secretions of the Amazon river frog *Lithobates palmipes* (Ranidae). *Comparative Biochemistry and Physiology - Part D: Genomics and Proteomics*, 2023, 46, pp.101069. 10.1016/j.cbd.2023.101069 . hal-04294874

HAL Id: hal-04294874

<https://hal.science/hal-04294874>

Submitted on 27 Nov 2023

HAL is a multi-disciplinary open access archive for the deposit and dissemination of scientific research documents, whether they are published or not. The documents may come from teaching and research institutions in France or abroad, or from public or private research centers.

L'archive ouverte pluridisciplinaire **HAL**, est destinée au dépôt et à la diffusion de documents scientifiques de niveau recherche, publiés ou non, émanant des établissements d'enseignement et de recherche français ou étrangers, des laboratoires publics ou privés.

1 **Peptidomic analysis of the host-defense peptides in skin secretions of the Amazon river**
2 **frog *Lithobates palmipes* (Ranidae)**

3

4 Milena Mechkarska^a, Gervonne Barran^a, Jolanta Kolodziejek^b, Laurent Coquet^{c,d},

5 Jérôme Leprince^e, Thierry Jouenne^c, Norbert Nowotny^b, J. Michael Conlon^{f*}

6

7 *^aDepartment of Life Sciences, The University of the West Indies, St Augustine, Trinidad and*

8 *Tobago*

9 *^bViral Zoonoses, Emerging and Vector-Borne Infections Group, Institute of Virology,*

10 *Department of Pathobiology, University of Veterinary Medicine, A-1210 Vienna, Austria*

11 *^cUniv Rouen Normandie, CNRS, INSA Rouen Normandie, PBS UMR 6270, F-76000 Rouen,*

12 *France*

13 *^dUniv Rouen Normandie, INSERM US51, CNRS UAR2026, HeRacLeS-PISSARO, F-76000*

14 *Rouen, France*

15 *^eInserm U982, PRIMACEN, Institute for Research and Innovation in Biomedicine (IRIB),*

16 *Normandy University, 76000 Mont-Saint-Aignan, France*

17 *^fDiabetes Research Centre, School of Biomedical Sciences, Ulster University, Coleraine*

18 *BT52 ISA, N. Ireland, U.K.*

19

20 **Corresponding author. Tel.: +44(0)7399435094; E-mail address: jmconlon1@gmail.com*

21 *(J.M. Conlon).*

22

23
24
25
26
27
28
29
30
31
32
33
34
35
36
37
38
39
40
41
42
43
44
45
46
47

ABSTRACT

Host-defense peptides synthesized in the skins of frogs are a source of potentially valuable therapeutic agents and their primary structures provide insight into the evolutionary history of species within a particular genus. Peptidomic analysis (~~reversed-phase HPLC combined with MALDI-TOF mass spectrometry and automated Edman degradation~~) was used to characterize the host-defense peptides in norepinephrine-stimulated skin secretions from the Amazon River frog *Lithobates palmipes* (Spix, 1824) collected in Trinidad. A total of ten peptides were purified and identified on the basis of amino acid similarity as belonging to the ranatuerin-2 family (ranatuerin-2PMa, -2PMb, -2PMc, and -2PMd), the brevinin-1 family (brevinin-1PMa, des(8-14)-1PMa, -1PMb, and -1PMc) and the temporin family (temporin-PMa in C-terminally amidated and non-amidated forms). Deletion of the sequence Val-Ala-Ala-Lys-Val-Leu-Pro from brevinin-1PMa in des(8-14)brevinin-1PMa resulted in a 10-fold decrease in potency against *Staphylococcus aureus* (MIC = 3 μ M compared with 31 μ M) and a >50-fold decrease in hemolytic activity. Temporin-PMa inhibited growth of *S. aureus* (MIC = 16 μ M) but the non-amidated form of the peptide lacked antimicrobial activity. Cladistic analysis based upon the primary structures of ranaturerin-2 peptides from New World frogs belonging to the genus *Lithobates* provides support for currently accepted phylogenetic relationships. A sister-group relationship between *L. palmipes* and Warszewitsch's frog *Lithobates warszewitschii* is indicated within a clade that included *Lithobates tarahumarae*.

Key words: host-defense peptide; antimicrobial, frog skin; brevinin-1, ranatuerin-2, temporin

48 1. Introduction

49

50 Host-defense peptides (HDPs) synthesized in the skins of a range of frog species comprise a
51 component of the animal's system of innate immunity, protecting against invasion by
52 pathogenic microorganisms in the environment (Varga et al., 2019). In addition, they may
53 facilitate the action of myotropic peptides in the secretions, such as bradykinins and
54 tachykinins, and other toxins to provide a defense against predators (Raaymakers et al.,
55 2017). Frog skin HDPs have excited interest as a source of potentially valuable therapeutic
56 agents. Although their growth-inhibitory activity against bacteria and fungi, including
57 antibiotic-resistant strains, has been the most extensively studied (Xu and Lai, 2015; Talapko
58 et al., 2022), HDPs are multifunctional and other potentially important clinically relevant
59 properties include immunomodulatory, wound healing antioxidant, anti-viral, anti-cancer, and
60 anti-diabetic actions [reviewed in (Conlon et al., 2019; Haney et al., 2019)]. However, it must
61 be pointed out the initial promise of using the repository of biologically active peptides
62 present in the skins of frogs as a source of new drugs has yet to be fulfilled as no compound
63 derived from amphibian HDPs is currently in clinical practice.

64 Frog skin HDPs are characterized by a very high degree of variability in their primary
65 structures and comparisons of their amino acid sequences can be used to complement
66 analyses based upon comparisons of nucleotide sequences of genes to provide insight into the
67 evolutionary history of species within a particular genus. Such cladistic analysis has been
68 successfully applied to elucidation of phylogenetic relationships within the extensive families
69 Ranidae (Conlon et al., 2009; Mechkarska et al., 2019), Pipidae (Coquet et al., 2016) and
70 Leptodactylidae (Barran et al., 2020)

71 The taxonomy of frogs belonging to the Ranidae family has undergone a series of major
72 revisions in recent years. Analyses based upon molecular as opposed to morphological

73 criteria demonstrate that the former genus *Rana* Linnaeus, 1758, once regarded as a single
74 taxon encompassing all members of the Ranidae family, does not constitute a monophyletic
75 group (Frost et al, 2006; Pauly et al., 2009) with the result that many well-known species
76 have been reclassified. At the time of writing, current recommendations divide the family
77 Ranidae comprising 437 species into 27 genera with the genus *Rana* being retained for a
78 more restricted group of 58 species from Eurasia and North America. The genus *Lithobates*
79 currently comprises 51 species from North, Central and South America to southern Brazil
80 (Frost, 2023). The Amazon river Frog *Lithobates palmipes* (Spix,1824), also known as the
81 Amazon waterfrog is widely distributed in northern and Amazonian South America east of
82 the Andes with a population established in Trinidad (Murphy et al., 2018). Its occupies
83 tropical rainforests near permanent sources of water as is listed by the International Union for
84 Conservation of Nature's Red List of Threatened Species as a species of least concern in
85 view of its distribution and presumed large population (IUCN, 2023). However, in some
86 countries the frogs are threatened because of invasive frog species, habitat modifications or
87 consumption as food.

88 In this study, the the reversed-phase HPLC coupled with MALDI-TOF mass
89 spectrometry and the automated Edman degradation were used to purify and characterize the
90 array of HDPs present in norepinephrine-stimulated secretions of *L. palmipes* frogs collected
91 in Trinidad. The peptides are classified according to the generally accepted nomenclature
92 recommended for designating such peptides from the Ranidae (Conlon, 2008). They are
93 assigned to a particular peptide family on the basis of structural similarity to previously
94 described peptides. PM is used to denote the species of origin and peptides from paralogous
95 genes are differentiated by numerals e.g ranatuerin-2PMa and ranatuerin-2PMb

96

97 2. Experimental

98 2.1. Collection of skin secretions

99 All experiments with live animals were approved by the Wildlife Section, Forestry
100 Division, Trinidad (Special Game License issued on 21/06/2016) and the University of the
101 West Indies (UWI) Campus Ethics Committee (CEC234/07/16) and were carried out by
102 authorized investigators. Adult *L. palmipes* (n = 2, sex not determined; 56 g and 67 g body
103 weight; 84 mm and 85 mm snout-to-vent length) were collected at Saunders Trace/Trinity
104 Inniss Field, South Trinidad (10°09'53.5"N, 61°15'42.7"W) in September 2019. The animals
105 were kept in captivity at the Animal House of the Department of Life Sciences, UWI at 24 -
106 28°C with a 12 h light /12 h dark cycle and were fed on crickets. To obtain skin secretions,
107 each frog was injected via the dorsal lymph sac with norepinephrine hydrochloride (40
108 nmol/g body weight) and placed in distilled water (100 mL) for 15 min. The collected
109 solution was acidified by addition of concentrated hydrochloric acid (0.5 mL) and
110 immediately frozen.

111

112 2.2. Purification of the peptides

113

114 The solutions containing the secretions were pooled and passed at a flow rate of
115 approximately 2 mL/min through 8 Sep-Pak C-18 cartridges (Waters Associates, Milford,
116 MA, USA) connected in series. Bound material was eluted with acetonitrile/water/
117 trifluoroacetic acid (TFA) (70.0:29.9:0.1, v/v/v) and freeze-dried. The material was
118 redissolved in 0.1% (v/v) TFA/water (2 mL) and injected onto a semipreparative (1.0 cm x 25
119 cm) Vydac 218TP510 (C-18) reversed-phase HPLC column (Grace, Deerfield, IL, USA)
120 equilibrated with 0.1% (v/v) TFA/water at a flow rate of 2.0 mL/min. The concentration of

121 acetonitrile in the eluting solvent was raised to 21% (v/v) over 10 min and to 63% (v/v) over
122 60 min using linear gradients. Absorbance was monitored at 214 nm and fractions (1 min)
123 were collected using a BioRad 2110 fraction collector. Previous studies from the laboratory
124 involving a wide range of frog species and employing the same conditions of
125 chromatography displayed in Fig. 1 have shown that the retention times of host-defense
126 peptides with cytotoxicity against microorganisms and/or mammalian cells are invariably
127 >35 min. Consequently, the peptides within the peaks that were present in major abundance
128 with retention times > 35 min were subjected to further purification by successive
129 chromatographies on (1.0 cm x 25 cm) Vydac 214TP510 (C-4) and (1.0 cm x 25 cm) Vydac
130 208TP510 (C-8) columns. The concentration of acetonitrile in the eluting solvent was raised
131 from 21% to 56% (v/v) over 50 min. The flow rate was 2.0 mL/min.

132

133 2.3. *Structural characterization*

134

135 MALDI-TOF mass spectrometry was carried out using an UltrafleXtreme instrument (Bruker
136 Daltonik, Bremen, Germany). Full details of the procedure, including calibration of the
137 instrument with peptides of known molecular mass in the 1 - 4 kDa range, have been
138 provided (Conlon et al., 2018). The accuracy of mass determinations was < 0.02%. The
139 primary structures of the purified peptides were determined by automated Edman degradation
140 using an Applied Biosystems model 494 Procise sequenator (Applied Biosystems,
141 Courtaboeuf, France).

142

143 2.4. *Antimicrobial assays*

144 Reference strains of microorganisms were purchased from the American Type Culture
145 Collection (Rockville, MD, USA). Minimum inhibitory concentration (MIC) of the purified

146 peptides against ampicillin-resistant *Staphylococcus aureus* ATCC 12600 and *Escherichia*
147 *coli* ATCC 25922 were measured by standard microdilution methods (Clinical Laboratory
148 and Standards Institute, 2019) as previously described (Barran et al., 2020). Reproducibility
149 of the assays was monitored by parallel incubations with serial dilutions of ampicillin (*E.*
150 *coli*) and vancomycin (*S. aureus*).

151

152 2.5. Hemolysis assay

153

154 All procedures involving animals were approved by Ulster University Animal Ethics Review
155 Committee and were carried out in accordance with the UK Animals (Scientific Procedures)
156 Act 1986 and EU Directive 2010/63EU for animal experiments. Hemolytic activity against
157 erythrocytes from female National Institutes of Health (NIH) Swiss mice was determined as
158 previously described (Barran et al., 2020). Control incubations were carried out in parallel in
159 Krebs Ringer bicarbonate buffer only and in 0.1% v/v Triton X100-water in order to
160 determine the absorbance associated with 0% and 100% hemolysis, respectively. The LC₅₀
161 value was taken as the mean concentration of peptide producing 50% hemolysis in three
162 independent experiments.

163

164 2.6. Cladistic analysis

165

166 The primary structures of 47 ranatuerin-2 peptides isolated from 21 *Lithobates* species from
167 the New World were compared. The amino acid sequences are shown in Supplementary Fig.
168 1. An expanded data set included an additional 20 ranatuerin-2 primary structures from 7
169 New World species belonging to the genus *Rana*. The additional amino acid sequences are
170 shown in Supplementary Fig. 2. Phylogenetic analyses were conducted in MEGA X (Kumar

171 et al., 2018). The optimal phylogenetic tree was constructed using the neighbor-joining
172 method (Saitou and Nei, 1987). The evolutionary distances were computed using the Poisson
173 correction model (Zuckerkandl and Pauling, 1965) and are given as the number of amino acid
174 substitutions per site. All positions containing alignment gaps and missing amino acid
175 residues were only eliminated in pairwise sequence comparisons (pairwise deletion option).
176 The amino acid sequence of ranatuerin-2 from the European frog *Rana graeca* (Mechkarska
177 et al., 2019) was included as out-group to polarize the in-group taxa.

178

179 **3. Results**

180

181

182 *3.1. Purification of the peptides*

183 An aliquot representing 20% of the total amount of pooled skin secretions, after partial
184 purification on Sep-Pak C-18 cartridges, was chromatographed on a Vydac C-18
185 semipreparative reversed-phase HPLC column (Fig. 1). The prominent peaks designated 1- 8
186 were collected and subjected to further purification on semipreparative Vydac C-4 and C-8
187 columns. Subsequent structural analysis showed that peak 1 contained des[8-14]brevinin-
188 1PMa, peak 2 ranatuerin-2PMa + ranatuerin-2PMB, peak 3 ranatuerin-2PMc, peak 4
189 ranatuerin-2PMd, peak 5 temporin-PM non-amidated, peak 6 brevinin-1PMa, peak 7
190 temporin-1PM, and peak 8 brevinin-1PMb + brevinin-1PMc. The peptides were purified to
191 near homogeneity (purity > 98% as assessed by a symmetrical peak shape and mass
192 spectrometry) by further chromatography on semipreparative Vydac C-4 and Vydac C-8
193 columns. The methodology is illustrated by the partial separation of brevinin-1PMb and
194 brevinin-1-PMc on a Vydac C-4 column (Fig. 2A), followed by purification to near
195 homogeneity of brevinin-1PMc on a Vydac C-8 column (Fig. 2B). The yields of purified
196 peptides were (nmol): des(8-14)brevinin-1PMa, 39; ranatuerin-2PMa, 85; ranatuerin-2PMB,

197 16; ranatuerin-2PMc, 38; ranatuerin-2PMd, 27; brevinin-1PMa, 76; brevinin-1PMb,
198 47; brevinin-1PMc, 86; temporin-PMa non-amidated, 12; temporin-PMa, 24.

199

200 3.2. Structural characterization

201 The primary structures of the peptides isolated from *L. palmipes* skin secretions were
202 established by automated Edman degradation and their complete primary structures are
203 shown in Table 1. The molecular masses of the peptides, determined by MALDI-TOF mass
204 spectrometry, were consistent with the proposed structures and are also shown in Table 1.
205 The data indicate that the ranatuerin-2 and brevinin-1 peptides were isolated in the oxidized
206 (disulfide-bridged) forms and that the temporin peptides in both C-terminally α -amidated and
207 non-amidated forms.

208

209 3.3. Antimicrobial and cytotoxicity activities

210

211 As shown in Table 2, brevinin-1PMa showed potent growth inhibitory activity against an
212 ampicillin-resistant strain of the Gram-positive bacterium *S. aureus* (MIC = 3 μ M) and was
213 active against a reference strain of the Gram-negative bacterium *E. coli* (MIC = 50 μ M). The
214 corresponding MIC value for ampicillin was 2.5 μ g/mL (*E. coli*) and 2.5 μ g/mL for
215 vancomycin (*S. aureus*). The peptide was strongly hemolytic against mouse erythrocytes
216 (LC₅₀ = 4 μ M). The antimicrobial potency of des(8-14)brevinin-1PMa containing a
217 heptapeptide deletion decreased 10-fold against *S. aureus* relative to the full-length peptide
218 but potency against *E. coli* was not significantly different (MIC = 62.5 μ M). Hemolytic
219 activity was markedly reduced (> 50-fold). Temporin-PMa inhibited growth of *S. aureus*
220 (MIC = 15.6 μ M) and was strongly hemolytic (LC₅₀ = 8 μ M) but was inactive against *E. coli*
221 (MIC > 250 μ M). The non-amidated form of temporin-PMa lacked antimicrobial activity

222 against both *S. aureus* and *E. coli* (MIC > 250 μ M) and was weakly hemolytic (LC₅₀ = 110
223 μ M).

224

225 3.4. Cladistic analysis

226

227 The optimal phylogenetic tree based upon the amino acid sequences of 47 ranatuerin-2
228 peptides isolated from 21 New World species belonging to the genus *Lithobates* is shown in
229 Fig. 3. The tree is drawn to scale, with branch lengths in the same units as those of the
230 evolutionary distances used to infer the phylogenetic tree. The optimal phylogenetic tree
231 based upon an expanded data set that included an additional 20 ranatuerin-2 primary
232 structures from 7 New World species belonging to the genus *Rana* is shown in Fig. 4.

233

234 Discussion

235

236 In common with other New World frogs from the genus *Lithobates* [reviewed in (Conlon
237 et al., 2009a, Xu and Lai, 2015)], peptides belonging to the ranatuerin-2, brevinin-1 and
238 temporin families are present in norepinephrine-stimulated skin secretions of *L. palmipes* in
239 relatively high concentrations. These peptide families were first identified on the basis of
240 their antibacterial and antifungal activities but certain members also display cytotoxicities
241 against human tumor cells (Xiong et al., 2021), cytokine-mediated immunomodulatory
242 properties (Popovic et al., 2012) as well as showing therapeutic potential as anti-diabetic
243 agents by their ability to stimulate insulin release from BRIN-BD11 clonal β -cells
244 (Mechkarska et al., 2011). The brevinin-1 and ranatuerin-2 peptides are present in multiple
245 molecular forms whose primary structures are closely related (Table 1). It is noteworthy that
246 ranaturin-2PMa and ranatuerin-2PMb as well as ranaturin-2PMc and ranatuerin-2PMd differ

247 in structure from each other only by the substitutions of Gln by Glu at a single site. It is
248 unlikely that the Glu-containing peptides are generated artefactually by hydrolysis of the
249 side-chain amide group of Gln during the collection and purification procedures as both
250 peptides were obtained in high yield but it is unclear whether each peptide is a product of a
251 separate gene or whether *L. palmipes* skin contains an enzyme analogous to mammalian
252 glutaminase that effects deamidation *in vivo*.

253 Des(8-14)brevinin-1P_{Ma} and the non- α -amidated temporin-P_{Ma} contain structural
254 features not usually found in members of their respective families and so it was considered
255 worthwhile to investigate their cytotoxic properties. Frog skin HDPs that display
256 antimicrobial activities are, with few exceptions, cationic, lack stable secondary structure in
257 aqueous solutions but have the propensity to form a stable amphipathic α -helix in the
258 environment of a phospholipid vesicle or in a membrane-mimetic solvent (Haney et al., 2009;
259 Han et al., 2021). Their antimicrobial potencies are determined by complex interactions
260 between molecular charge, hydrophobicity, conformation (stability of the α -helix) and
261 amphipathicity (Chen et al., 2022). NMR studies have shown that peptides of the brevinin-1
262 family have the propensity to form a stable α -helical conformation in a membrane-mimetic
263 environment but the conformation is associated with a stable kink at the site of the conserved
264 Pro¹⁴ residue (Suh et al., 1999; Timmons et al., 2019). Abolition of this kink in brevinin-
265 1P_{Ra} (formerly termed gaegurin-5) by the substitution Pro \rightarrow Ala to produce a linear helix
266 resulted in a decrease in antimicrobial potency (Park et al., 2002), suggesting that this
267 structural feature is important in disrupting the integrity of the bacterial cell membrane
268 (Kabelka and Vácha, 2021). Brevinin-1P_{Ma} is strongly cationic (net charge at pH 7 = +4)
269 and is associated with a high degree of hydrophobicity (H = 0.762) (Fauchere and Pliska,
270 1983). The hydrophobic moment μ H, a semi-quantitative measure of the degree of
271 amphipathicity (Eisenberg et al., 1982) is 0.331. The atypical brevinin-1 peptide, (des(8-

272 14)brevinin-1PMa (FLPLIAGKIFCA ISKKC) contains the heptapeptide deletion Val⁸-Ala⁹-
273 Ala¹⁰-Lys¹¹-Val¹²-Leu¹³-Pro¹⁴ compared with brevinin-1PMa, resulting in a decrease in
274 cationicity to +3 but the peptide maintains high hydrophobicity (H = 0.811) and
275 amphipathicity (μ H = 0.276). Des(8-14)brevinin-1PMa displayed markedly decreased
276 potency against *S. aureus* (10-fold) and an even greater reduction in hemolytic activity (>50-
277 fold) relative to the full-length peptide which may be a consequence of both the reduced
278 cationicity and the absence of the kink-producing Pro¹⁴ residue.

279 The temporins are small (8 - 17 amino acid residues), C-terminally α -amidated
280 peptides that are widely distributed in ranid frogs of both Eurasian and N. American origin.
281 With the exception of the broad spectrum temporin L (Bellavita et al., 2022), they display
282 varying degrees of growth-inhibitory activity against Gram-positive bacteria but are inactive
283 against Gram-negative bacteria. The temporins show possibility for development into anti-
284 infective agents, especially in view of the fact that, lacking a cystine bridge, they are easy to
285 synthesize (Mangoni et al., 2016). However, the therapeutic potential of temporin-PMa, like
286 that of brevinin-1PMa is limited by the fact that the peptides are strongly hemolytic. The
287 reduction in cationicity from +2 to +1 at pH 7 in the non-amidated form of temporin-PMa
288 compared with the α -amidated form, resulted in abolition of antimicrobial activity against *S.*
289 *aureus* and a substantial decrease in hemolytic activity ($LC_{50} = 110 \mu$ M compared with 8μ M
290 for the α -amidated form).

291 Comparisons of the primary structures of host-defense peptides from amphibian
292 species within a particular genus have proved valuable in elucidation phylogenetic
293 relationships and evolutionary histories within that genus (Conlon et al., 2009a). The primary
294 structures of ranatuerin-2 peptides have been poorly conserved between species so that the
295 peptide represents a useful probe to investigate phylogenetic relationships within the genus
296 *Lithobates*. The present study involves an extension of an early cladistic analysis based upon

297 the primary structures of ranatuerin-2 peptides that used a more limited data set (Conlon et
298 al., 2014). The data are consistent with the earlier analysis and result in a phylogenetic tree
299 whose features generally support currently accepted evolutionary relationships based upon
300 morphological criteria and the nucleotide sequence of paralogous genes (Fig.3). *L. palmipes*
301 is placed as sister-group to Warszewitsch's frog *Lithobates warszewitschii* (Conlon et al.,
302 2009b) in a clade that also contains the Tarahumare frog *Lithobates tarahumarae* (Rollins-
303 Smith et al., 2002). It is noteworthy that the bullfrogs *Lithobates catesbeianus*, *Lithobates*
304 *clamitans*, *Lithobates grylio*, *Lithobates heckscheri*, *Lithobates okaloosae*, *Lithobates*
305 *septentrionalis* and *Lithobates virgatipes*, formerly classified in the Aquarana species group
306 of Hillis and Wilcox (2005), segregate in a distinct and well-defined clade. Expanding the
307 data set to include an additional 20 ranatuerin-2 primary structures from 7 New World
308 species belonging to the genus *Rana*, does not alter the proposed sister-group relationship
309 between *L. palmipes* and *L. warszewitschii*. *Rana aurora*, *Rana boylii*, *Rana cascadae*, *Rana*
310 *draytonii*, *Rana luteiventris*, *Rana muscosa* and *Rana pretiosa* segregate together in a well-
311 defined clade, thereby providing support for a taxonomic classification in which N. American
312 Ranidae are arranged in the distinct genera *Lithobates* and *Rana*.

313 Peptidomic analyses of skin secretions have also been used to characterize different
314 population clusters of the same species. For example, the methodology described in the
315 present study has provided firm evidence that the N. American red-legged frogs, *Rana aurora*
316 *draytonii* and *Rana aurora aurora* (Conlon et al., 2006) and the Japanese frogs *Rana tagoi*
317 *okiensis* and *Rana tagoi tagoi* (Conlon et al., 2010) are distinct species. In contrast, similar
318 analysis suggested that morphologically distinct populations of the Chiricahua leopard frog
319 *Lithobates chiricahuensis* occupying regions in southern Arizona and those from the
320 Mogollon Rim of central Arizona are probably conspecific (Conlon et al., 2011). As
321 Trinidad is separated from the northeast coast of Venezuela by only 11 km, it will be

322 worthwhile to compare the skin peptidome of *L. palmipes* from Trinidad determined in this
323 study with that of frogs from the population in the coastal region of Venezuela in order to
324 determine whether they should be regarded as sub-species. If *L. palmipes* from Trinidad
325 emerges as a distinct lineage it will represent a clear example of allopatric speciation.

326

327 **Acknowledgements**

328 Experimental work was supported by a CR&P grant (CRP.5.OCT18.66) and travel grant
329 (CRP.5.OCT19.94) for visiting Ulster University awarded to GB from the School for
330 Graduate Studies and Research University of the West Indies, St. Augustine Campus.

331

332 **REFERENCES**

333

334 Barran, G., Kolodziejek, J., Coquet, L., Leprince, J., Jouenne, T., Nowotny, N., Conlon, J.M.,
335 Mechkarska, M., 2020. Peptidomic analysis of skin secretions of the Caribbean frogs
336 *Leptodactylus insularum* and *Leptodactylus nesiotus* (Leptodactylidae) identifies an
337 ocellatin with broad spectrum antimicrobial activity. *Antibiotics (Basel)* 9, 718.

338 Bellavita, R., Buommino, E., Casciaro, B., Merlino, F., Cappiello, F., Marigliano, N.,
339 Saviano, A., Maione, F., Santangelo, R., Mangoni, M.L., Galdiero, S., Grieco, P.,
340 Falanga, A., 2022. Synthetic amphipathic β -Sheet temporin-derived peptide with dual
341 antibacterial and anti-inflammatory activities. *Antibiotics (Basel)* 11, 1285.

342 Chen, X., Liu, S., Fang, J., Zheng, S., Wang, Z., Jiao, Y., Xia, P., Wu, H., Ma, Z., Hao, L.,
343 2022. Peptides isolated from amphibian skin secretions with emphasis on antimicrobial
344 peptides. *Toxins* 14, 722.

345 Clinical Laboratory and Standards Institute. *Methods for Dilution Antimicrobial*
346 *Susceptibility Tests for Bacteria That Grow Aerobically*, 11th ed.; Approved Standard
347 M07; CLSI: Wayne, PA, USA, 2019.

348 Conlon, J.M., 2008. Reflections on a systematic nomenclature for antimicrobial peptides
349 from the skins of frogs of the family Ranidae. *Peptides* 29, 1815-1819.

350 Conlon, J.M., Al-Ghaferi, N., Coquet, L., Leprince, J., Jouenne, T., Vaudry, H., Davidson,
351 C., 2006. Evidence from peptidomic analysis of skin secretions that the red-legged frogs,
352 *Rana aurora draytonii* and *Rana aurora aurora* are distinct species. *Peptides* 27, 1305-
353 1312.

354 Conlon, J.M., Kolodziejek, J., Nowotny, N., 2009a. Antimicrobial peptides from the skins of
355 North American frogs. *Biochim. Biophys. Acta* 1788, 1556-1563.

356 Conlon, J.M., Meetani, M.A., Coquet, L., Jouenne, T., Leprince, J., Vaudry, H., Kolodziejek,
357 J., Nowotny, N., King, J.D., 2009b. Antimicrobial peptides from the skin secretions of
358 the New World frogs *Lithobates capito* and *Lithobates warszewitschii* (Ranidae).
359 Peptides. 30, 1775-1781.

360 Conlon, J.M., Coquet, L., Jouenne, T., Leprince, J., Vaudry, H., Iwamuro, S., 2010. Evidence
361 from the primary structures of dermal antimicrobial peptides that *Rana tagoi okiensis* and
362 *Rana tagoi tagoi* (Ranidae) are not conspecific subspecies. Toxicon 55, 430-435.

363 Conlon, J.M., Mechkarska, M., Coquet, L., Jouenne, T., Leprince, J., Vaudry, H.,
364 Kolodziejek, J., Nowotny, N., King, J.D., 2011. Characterization of antimicrobial
365 peptides in skin secretions from discrete populations of *Lithobates chiricahuensis*
366 (Ranidae) from central and southern Arizona. Peptides 32, 664-669.

367 Conlon, J.M., Kolodziejek, J., Mechkarska, M., Coquet, L., Leprince, J., Jouenne, T., Vaudry,
368 H., Nielsen, P.F., Nowotny, N., King, J.D., 2014. Host defense peptides from *Lithobates*
369 *forreri*, *Hylarana luctuosa*, and *Hylarana signata* (Ranidae): phylogenetic relationships
370 inferred from primary structures of ranatuerin-2 and brevinin-2 peptides. Comp.
371 Biochem. Physiol. Part D Genomics Proteomics 9, 49-57.

372 Conlon, J.M., Moffett, R.C., Leprince, J., Flatt, P.R., 2018. Identification of components in
373 frog skin secretions with therapeutic potential as antidiabetic agents. Methods Mol. Biol.
374 1719, 319-333.

375 Conlon, J.M., Mechkarska, M., Leprince, J., 2019. Peptidomic analysis in the discovery of
376 therapeutically valuable peptides in amphibian skin secretions. Expert Rev. Proteomics
377 16, 897-908.

378

379

380 Coquet, L., Kolodziejek, J., Jouenne, T., Nowotny, N., King, J.D., Conlon, J.M., 2016.
381 Peptidomic analysis of the extensive array of host-defense peptides in skin secretions of
382 the dodecaploid frog *Xenopus ruwenzoriensis* (Pipidae). *Comp. Biochem. Physiol. Part D*
383 *Genomics Proteomics*. 19, 18-24.

384 Eisenberg, D., Weiss, R.M., Terwilliger, T.C., 1982. The helical hydrophobic moment: a
385 measure of the amphiphilicity of a helix. *Nature*, 299, 371–374.

386 Fauchere, J., Pliska, V., 1983. Hydrophobic parameters { π } of amino-acid side chains from
387 the partitioning of N-acetyl-amino-acid amides. *Eur. J. Med. Chem.* 8, 369–375.

388 Frost, D.R., 2023. Amphibian Species of the World: an Online Reference. Version 6.1.
389 (accessed January 2023) Electronic Database accessible at
390 <https://amphibiansoftheworld.amnh.org/index.php>. American Museum of Natural
391 History, New York, USA.

392 Frost, D.R., Grant, T., Faivovich, J., Bain, R.H., Haas, A., Haddad, C.F.B., De Sa, R.O.,
393 Channing, A., Wilkinson, M., Donnellan, S.C., Raxworthy, C.J., Campbell, J.A., Blotto,
394 B.L., Moler, P., Drewes, R.C., Nussbaum, R.A., Lynch, J.D., Green, D.M., Wheeler,
395 W.C., 2006. The amphibian tree of life. *Bull. Am. Mus. Nat. His.* 297, 1-370.

396 Han, Y., Zhang, M., Lai, R., Zhang, Z., 2021. Chemical modifications to increase the
397 therapeutic potential of antimicrobial peptides. *Peptides* 146, 170666.

398 Haney, E.F., Hunter, H.N., Matsuzaki, K., Vogel, H.J., 2009. Solution NMR studies of
399 amphibian antimicrobial peptides: linking structure to function? *Biochim Biophys Acta*.
400 1788, 1639-1655.

401 Haney, E.F., Straus, S.K., Hancock, R.E.W., 2019. Reassessing the host defense peptide
402 landscape. *Front. Chem.* 7, 43.

403 Hillis, D.M., Wilcox, T.P., 2005. Phylogeny of the New world true frogs (*Rana*). Mol.
404 Phylogenet. Evol. 34, 299-314.

405 International Union for Conservation of Nature Red List of Threatened Species, Version
406 2021-3, accessed January 2023, 2023. <https://www.iucnredlist.org>.

407 Kabelka, I., Vácha, R., 2021. Advances in molecular understanding of α -helical membrane-
408 active peptides. Acc. Chem. Res. 54, 2196-2204.

409 Kumar, S., Stecher, G., Li, M., Knyaz, C., Tamura, K., 2018. MEGA X: Molecular
410 Evolutionary Genetics Analysis across computing platforms. Mol. Biol. Evol. 35, 1547–
411 1549.

412 Mangoni, M.L., Grazia, A.D., Cappiello, F., Casciaro, B., Luca V., 2016. Naturally occurring
413 peptides from *Rana temporaria*: antimicrobial properties and more. Curr. Top. Med.
414 Chem. 16, 54-64.

415 Mechkarska, M., Ojo, O.O., Meetani, M.A., Coquet, L., Jouenne, T., Abdel-Wahab, Y.H,
416 Flatt, P.R., King, J.D., Conlon, J.M., 2011. Peptidomic analysis of skin secretions from
417 the bullfrog *Lithobates catesbeianus* (Ranidae) identifies multiple peptides with potent
418 insulin-releasing activity. Peptides 32, 203-208.

419 Mechkarska, M., Kolodziejek, J., Musale, V., Coquet, L., Leprince, J., Jouenne, T., Nowotny,
420 N., Conlon, J.M., 2019. Peptidomic analysis of the host-defense peptides in skin
421 secretions of *Rana graeca* provides insight into phylogenetic relationships among
422 Eurasian *Rana* species. Comp. Biochem. Physiol. Part D Genomics Proteomics 29, 228-
423 234.

424 Murphy, J.C., Downie, J.R., Smith, J.M., Livingstone, S.R., Mohammed, R.S., Auguste, R.J.,
425 Lehtinen, R.M., Eyre, M., Sewlal, J.N., Noriega, N., Casper, G.S., Anton, T., Thomas,
426 R.A., Rutherford, M.G., Braswell, A.L., Jowers, M.J., 2018. A Field Guide to the

427 Amphibians & Reptiles of Trinidad & Tobago. Trinidad and Tobagos Field Naturalist's
428 Club. ISBN-978-976-8255-47-1.

429 Park, S.H., Kim, H.E., Kim, C.M., Yun, H.J., Choi, E.C., Lee, B.J., 2002. Role of proline,
430 cysteine and a disulphide bridge in the structure and activity of the anti-microbial peptide
431 gaegurin 5. *Biochem J.* 368(Pt 1), 171-182.

432 Pauly, G.B., Hillis, D.M., Cannatella, D.C., 2009. Taxonomic freedom and the role of official
433 lists of species names. *Herpetologica* 65, 115-28.

434 Popovic, S., Urbán, E., Lukic, M., Conlon, J.M., 2012. Peptides with antimicrobial and anti-
435 inflammatory activities that have therapeutic potential for treatment of *acne vulgaris*.
436 *Peptides* 34, 275-282.

437 Raaymakers, C., Verbrugghe, E., Hernot, S., Hellebuyck, T., Betti, C., Peleman, C., Claeys,
438 M., Bert, W., Caveliers, V., Ballet, S., Martel, A., Pasmans, F., Roelants, K., 2017.
439 Antimicrobial peptides in frog poisons constitute a molecular toxin delivery system
440 against predators. *Nat. Commun.* 8, 1495.

441 Rollins-Smith, L.A., Reinert, L.K., Miera, V., Conlon, J.M., 2002. Antimicrobial peptide
442 defenses of the Tarahumara frog, *Rana tarahumarae*. *Biochem. Biophys. Res. Commun.*
443 297, 361-367.

444 Saitou, N., Nei, M., 1987. The neighbor-joining method: A new method for reconstructing
445 phylogenetic trees. *Mol. Biol. Evol.* 4, 406-425.

446 Suh, J.Y., Lee, Y.T., Park, C.B., Lee, K.H., Kim, S.C., Choi, B.S., 1999. Structural and
447 functional implications of a proline residue in the antimicrobial peptide gaegurin. *Eur. J.*
448 *Biochem.* 266, 665-674.

449 Talapko, J., Meštrović, T., Juzbašić, M., Tomas, M., Erić, S., Horvat Aleksijević, L., Bekić,
450 S., Schwarz, D., Matic, S., Neuberg, M., Škrlec, I.. Antimicrobial peptides-mechanisms
451 of action, antimicrobial effects and clinical applications. *Antibiotics (Basel)* 11, 1417.

452 Timmons, P.B., O'Flynn, D., Conlon, J.M., Hewage, C.M., 2019. Structural and positional
453 studies of the antimicrobial peptide brevinin-1BYa in membrane-mimetic environments.
454 J. Pept. Sci. 25, e3208.

455 Varga, J.F.A., Bui-Marinou, M.P., Katzenback, B.A., 2019. Frog skin innate immune
456 defences: sensing and surviving pathogens. Front. Immunol. 9, 3128.

457 Xiong, S., Wang, N., Liu, C., Shen, H., Qu, Z., Zhu, L., Bai, X., Hu, H.G., Cong, W., Zhao,
458 L., 2021. Design, synthesis, and anti-tumor activities of novel brevinin-1BYa
459 peptidomimetics. Bioorg. Med. Chem. Lett. 37, 127831.

460 Xu, X., Lai, R., 2015. The chemistry and biological activities of peptides from amphibian
461 skin secretions. Chem. Rev. 115, 1760–1846.

462 Zuckerkandl, E., Pauling, L., 1965. Evolutionary divergence and convergence in proteins. In:
463 Bryson, V, and Vogel, H.J., editors. Evolving Genes and Proteins. New York: Academic
464 Press; p. 97-166.

465

466

467 **Legend to Figures**

468

469 Fig. 1. Reversed-phase HPLC on a semipreparative Vydac C-18 column of pooled skin
470 secretions from two *L. palmipes* frogs collected in Trinidad after partial purification on Sep-
471 Pak C-18 cartridges. The dashed line shows the concentration of acetonitrile in the eluting
472 solvent. The peaks denoted 1-8 contain host-defense peptides that were purified further.

473

474 Fig. 2. (A) Separation of brevinin-1PMb and brevinin-1PMc on a semipreparative Vydac C-4
475 column and (B) purification to near homogeneity of brevinin-1PMb on a semipreparative
476 Vydac C-8 column. The arrowheads show where peak collection began and ended. The
477 dashed line shows the concentration of acetonitrile in the eluting solvent.

478

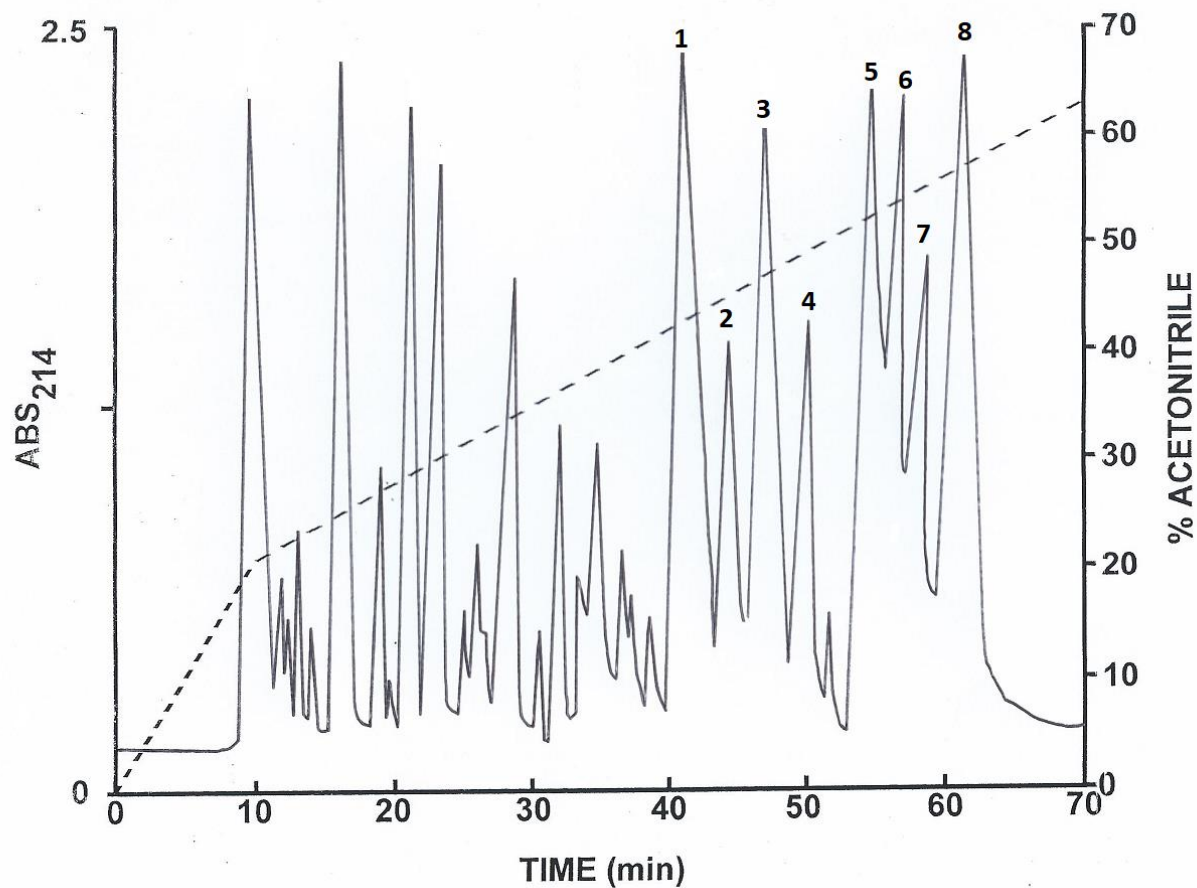
479

480 Fig. 3. A phylogenetic tree generated using the neighbor-joining method with Poisson
481 correction based upon the primary structures of the ranatuerin-2 peptides isolated from New
482 World frogs belonging to the genus *Lithobates*.

483

484 Fig. 4. A phylogenetic tree generated using the neighbor-joining method with Poisson
485 correction based upon the primary structures of the ranatuerin-2 peptides isolated from New
486 World frogs belonging to the genera *Lithobates* and *Rana*.

487

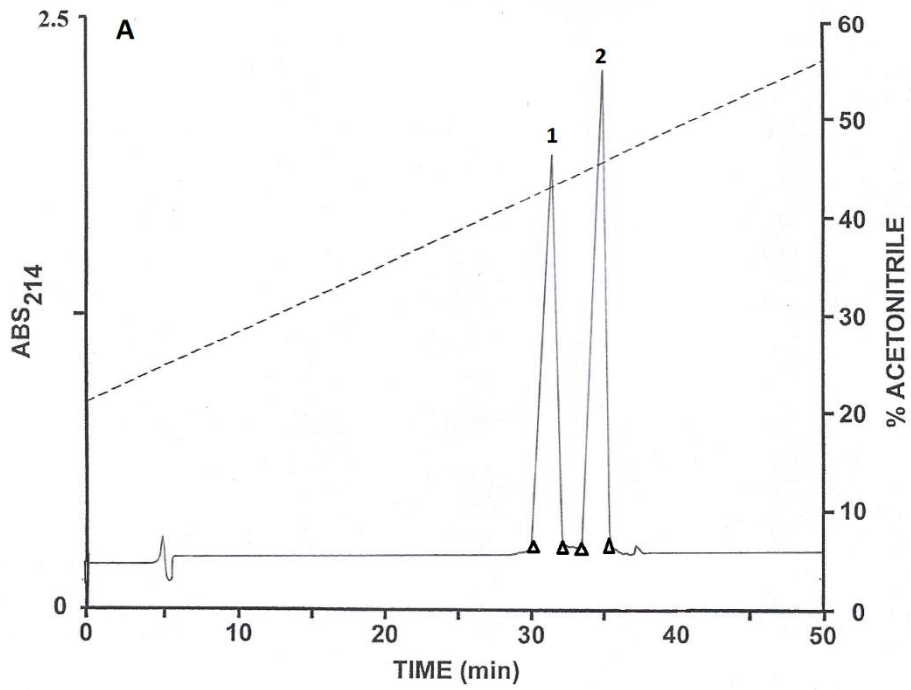


488

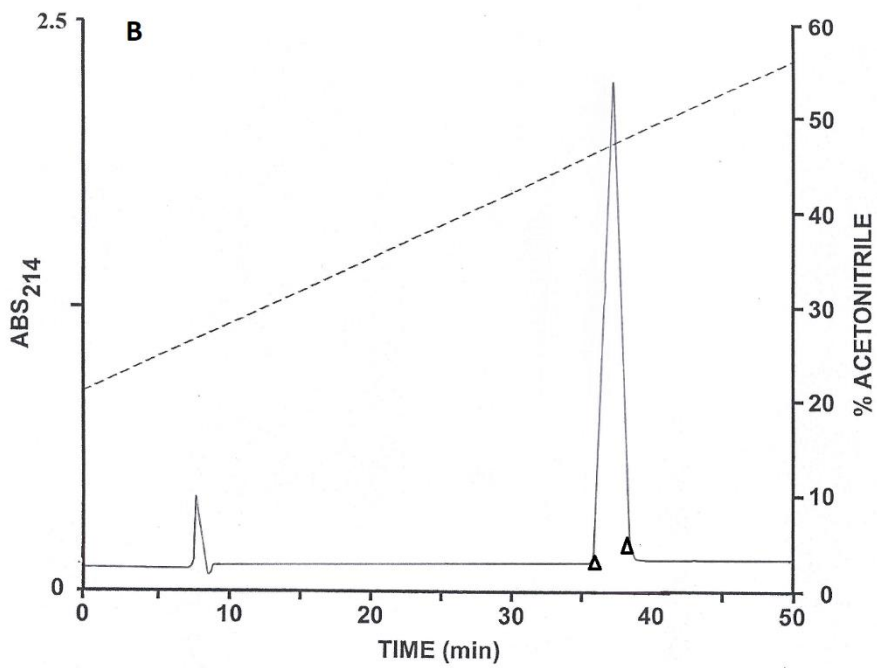
489

490 Fig. 1

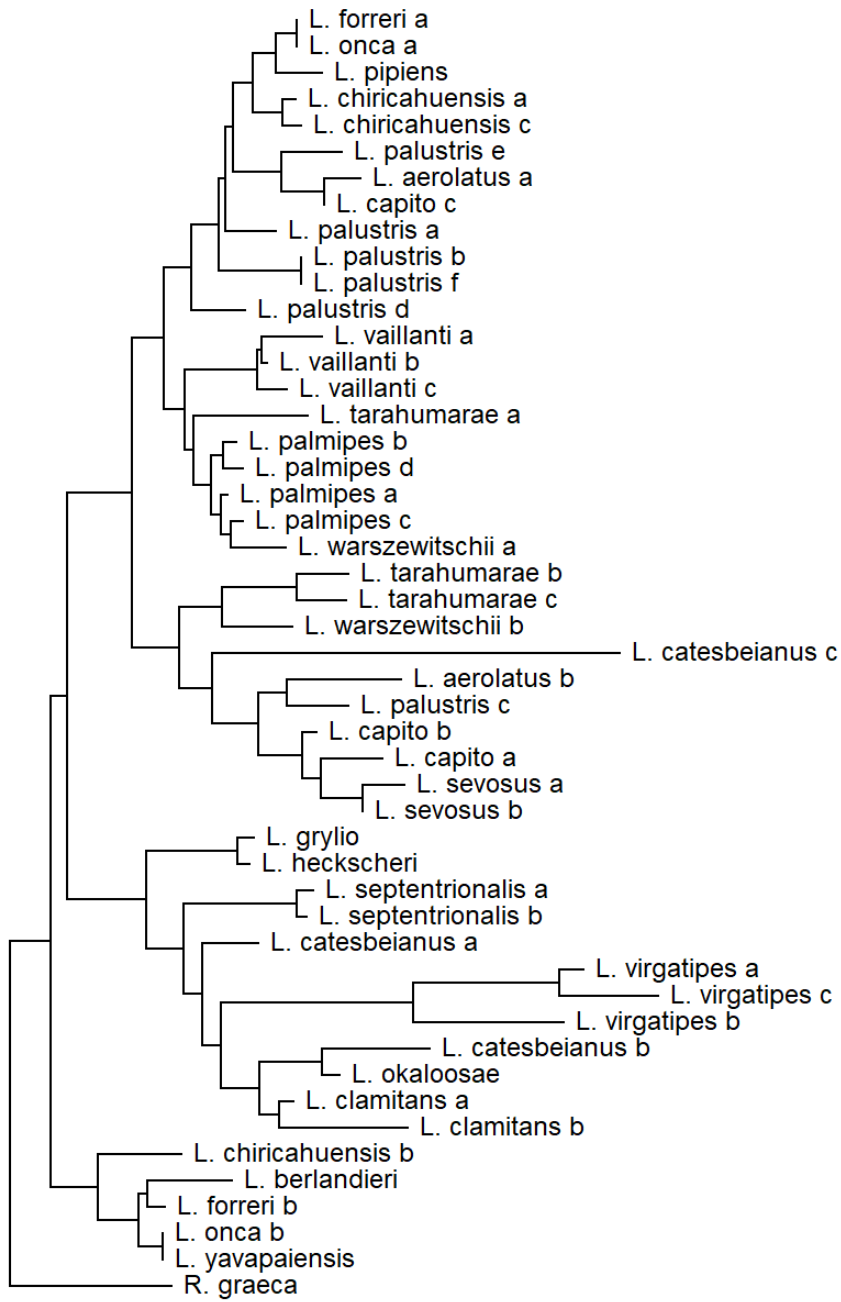
491



492
493



494
495
496 Fig. 2
497

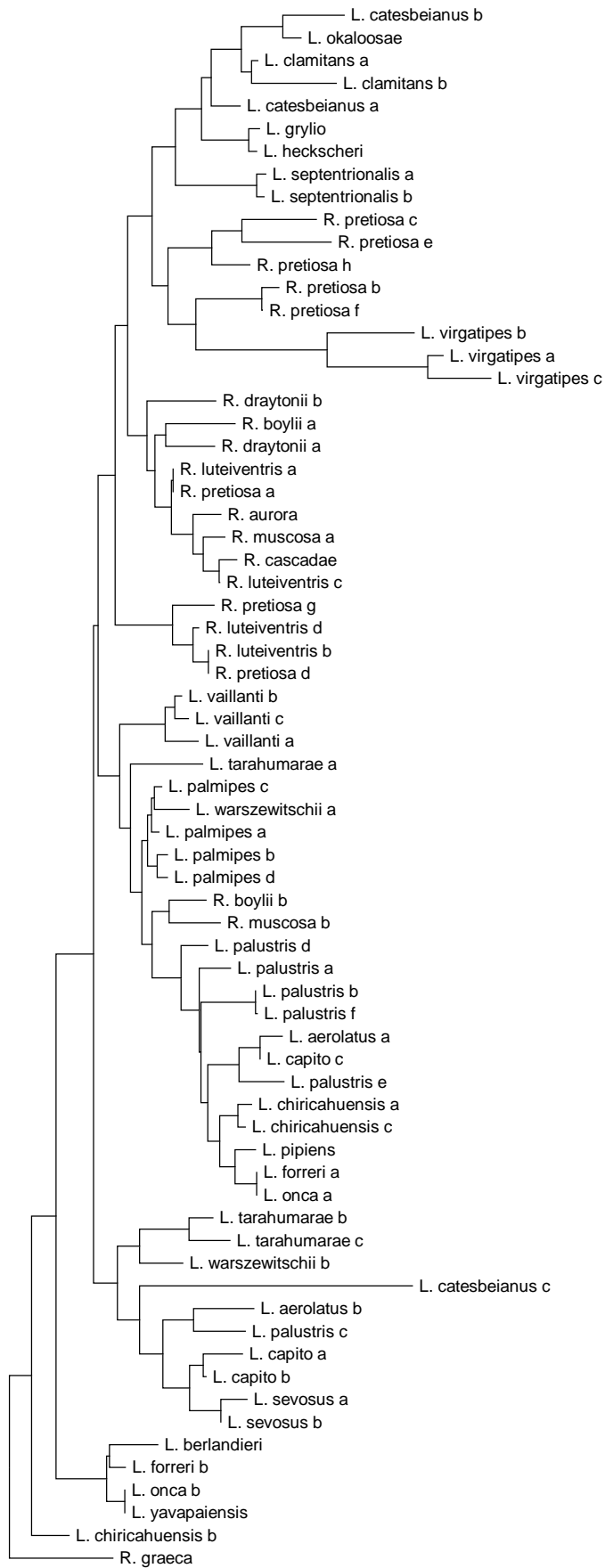


0.10

498

499

500 Fig. 3



502 Table 1. Primary structures and molecular masses of the peptides isolated from
 503 norepinephrine stimulated skin secretions from *L. palmipes*.

Peak	Peptide	Primary Structure	[MH ⁺] _{calc}	[MH ⁺] _{obs}
1	Des (8-14) brevinin-1P _{Ma}	FLPLIAGKIFCAISKKC	1850.1	1850.0
2	Ranatuering-2P _{Ma}	GIMDSIKGAAKNLAGQLLDKLGKCKITGC	2887.6	2887.4
2	Ranatuering-2P _{Mb}	GIMDSIKGAAKNLAGELLDKLGKCKITGC	2888.6	2888.4
3	Ranatuering-2P _{Mc}	GIMDSIKGVAKNLGQLLDKLGKCKITGC	2915.6	2915.3
4	Ranatuering-2P _{Md}	GIMDSIKGVAKNLGELLDKLGKCKITGC	2916.6	2916.4
5	Temporin-P _{Ma} non-amidated	FLPFLGKLLSGIF	1451.8	1451.5
6	Brevinin-1P _{Ma}	FLPLIAGVAAKVLPKIFCAISKKC	2528.5	2528.5
7	Temporin-P _{Ma}	FLPFLGKLLSGIF ^a	1450.8	1450.5
8	Brevinin-1P _{Mb}	FLPLIAGMAANFLPKIFCAISKKC	2594.4	2594.4
8	Brevinin-1P _{Mc}	FLPIIAGVAAKVLPKVFCFITKKC	2604.5	2604.5

504
 505 ^a denotes C-terminal α-amidation. Peak number refers to Fig. 1 and [MH⁺]_{obs} denotes
 506 observed molecular mass and [MH⁺]_{calc} denotes the mass calculated from the proposed
 507 structures.

508
 509
 510
 511
 512
 513
 514
 515

516 Table 2. Minimum inhibitory concentration (MIC) and hemolytic activity against mouse red
517 blood cells (R.B.C.) of peptides isolated from skin secretions of the Amazon River frog *L.*
518 *palmipes*

519

Peptide	MIC (μ M) <i>E. coli</i>	MIC (μ M) <i>S. aureus</i>	LC ₅₀ (μ M) R.B.C.
Des[8-14]brevinin-1PMa	62.5	31.3	>200
Brevinin-1PMa	50	3.1	4
Temporin-PMa	>250	15.6	8
Temporin-PMa non-amidated	>250	>250	110

520

521

522

523 *L. aerolatus* a GL*MDTVKNAAKNLA****GQLLDTIKCKMTG*C
524 *L. aerolatus* b GI*LDTIKNAAKTVA****VGLLEKIKCKMTG*C
525 *L. berlandieri* GL*LDTIKGVAKTVA****ASMLDKLKCKISG*C
526 *L. capito* a GI*MDTIKDTAKTVA****VGLLDKIKCTITG*C
527 *L. capito* b GI*MDTIKNTAKTVA****VGLLDKIKCKITG*C
528 *L. capito* c GL*MDTVKNAAKNLA****GQLLDTIKCKITG*C
529 *L. catesbeianus* a GLFLDTLKGAAKDVA****GK*LEGLKCKITG*CKLP
530 *L. catesbeianus* b GVFLDTLKGLAGKM*****LESKCKIAG*CKP
531 *L. catesbeianus* c GF*LDI IKNLGKTFA****GHMLDKIKCTIGT*CPPSP
532 *L. chiricahuensis* a GL*MDTVKNAAKNLA****GQLLDRLKCKITG*C
533 *L. chiricahuensis* b GL*MDTIKGVAKNVA****ASLLEKIKCKVTG*C
534 *L. chiricahuensis* c GL*MDTVKNVAKNLA****GQLLDRLKCKITG*C
535 *L. clamitans* a GLFLDTLKGAAKDVA****GKLEGLKCKIAG*CKP
536 *L. clamitans* b GLFLDTLKG****LA****GKLLQGLKCIKAG*CKP
537 *L. forreri* a GL*MDTVKNAAKNLA****GQMLDKLKCKITG*C
538 *L. forreri* b GL*MDTVKGVAKTVA****ASMLDKLKCKITG*CKTT
539 *L. grylio* GLLLDTLKGAAKDIA****GIALEKIKCKITG*CKP
540 *L. heckscheri* GLFLDTLKGAAKDIA****GIALEKIKCKITG*CKP
541 *L. okaloosae* GLFVDTLKG****LA****GKMLESKCKIAG*CKP
542 *L. onca* a GL*MDTVKNAAKNLA****GQMLDKLKCKITGSC
543 *L. onca* b GL*MDTIKGVAKTVA****ASWLDKIKCKITG*C
544 *L. palmipes* a GI*MDSIKGAAKNLA****GQLLDKIKCKITG*C
545 *L. palmipes* b GI*MDSIKGAAKNLA****GELLDKIKCKITG*C
546 *L. palmipes* c GI*MDSIKGVAKNLA****GQLLDKIKCKITG*C
547 *L. palmipes* d GI*MDSIKGVAKNLA****GELLDKIKCKITG*C
548 *L. palustris* a GI*MDTVKNVAKNLA****GQLLDKIKCKITA*C
549 *L. palustris* b GI*MDTVKNAAKDLA****GQLLDKIKCKRITG*C
550 *L. palustris* c GL*LDTIKNTAKNLA****VGLLDKIKCKMTG*C
551 *L. palustris* d GI*MDSVKNVAKNIA****GQLLDKIKCKITG*C
552 *L. palustris* e GI*MDSVKNAAKNLA****GQLLDTIKCKITA*C
553 *L. palustris* f GI*MDTVKNAAKDLA****GQ*LDKIKCKRITG*C
554 *L. pipiens* GL*MDTVKNVAKNLA****GHMLDKIKCKITG*C
555 *L. septentrionalis* a GLFLNTVKDVAKDVAKDVAGKLLLESKCKITG*CKS
556 *L. septentrionalis* b GLFLNTVKDVAKDVAKDVAGKLLLESKCKITG*CKP
557 *L. sevosus* a AI*MDTIKDTAKTVA****VGLLNKIKCKITG*C
558 *L. sevosus* b GI*MDTIKDTAKTVA****VGLLNKIKCKITG*C
559 *L. tarahumarae* a GI*MDSIKGAAKEIA****GHLLDNLKCKITG*C
560 *L. tarahumarae* b GI*LDTLKNVAKNVA****AGLLDNIKCKITG*C
561 *L. tarahumarae* c GI*FDTIKNVAKNMA****AGLLDNIKCKITG*C
562 *L. vaillantii* a GI*MDTIKGAAKDVA****AQLLDKIKCKITK*C
563 *L. vaillantii* b GI*MDTIKGAAKDLA****GQLLDKIKCKITK*C
564 *L. vaillantii* c GI*MDTIKGAAKDLA****GELLDKIKCKITK*C
565 *L. virgatipes* a GVFLDTLKGVGKDA****VKLLEALQCKFGV*CKN
566 *L. virgatipes* b GVFLDALKGVGKVA****VSLLNGLKCKLGV*C
567 *L. virgatipes* c GVFLNTIKEVGKDA****VKLLEALQCKFGV*CKT
568 *L. warszewitschii* a GI*MDSIKGLGKNLA****GQLLDKIKCKITG*C
569 *L. warszewitschii* b GL*FDSIKNVAKNVA****AGLLDKIKCKITG*C
570 *L. yavapaiensis* GL*MDTIKGVAKTVA****ASWLDKIKCKITG*C
571 *R. aurora* GI*LSSFKGVAKGVAKNLAGKLLDELKCKITG*C
572 *R. boylii* a GI*LSTFKGLAKGVAKDLAGNLLDKFKCKITG*C
573 *R. boylii* b GI*MDSVKGLAKNLA****GKLLDSLKCKITG*C

574 *R. graeca* GL*MDVVKGAAKNLF***AAALEKCLKCKVTG*C

575

576 Supplementary Fig. 1. Primary structures of 47 ranatuerin-2 peptides isolated from 21

577 *Lithobates* species from the New World. In order to maximize structural similarity, amino

578 acid gaps denoted by * have been introduced into some sequences.

579

580

581	<i>R. aurora</i>	GILSSFKGVAKGVAKNLAGKLLDELKCKITGC
582	<i>R. boylei</i> a	GILSTFKGLAKGVAKDLAGNLLDKFKCKITGC
583	<i>R. boylei</i> b	GIMDSVKGLAKNLA****GKLLDSLKCKITGC
584	<i>R. cascadae</i>	GILSSFKGVAKGVAKDLAGKLLLETLKCKITGC
585	<i>R. draytonii</i> a	GIMDTFKGVAKGVAKDLAVKLLDNFKCKITGC
586	<i>R. draytonii</i> b	GIMDTFKGIKGVAKNLAGKLLDELKCKMTGC
587	<i>R. luteiventris</i> a	GILDSFKGVAKGVAKDLAGKLLDKLKCKITGC
588	<i>R. luteiventris</i> b	GILSSIKGVAKGVAKNVAAQLLDTLKCKITGC
589	<i>R. luteiventris</i> c	GILSSFKGVAKGVAKDLAGKLLDTLKCKITGC
590	<i>R. luteiventris</i> d	GILSSIKGVAKNVA****AQLLDTLKCKITGC
591	<i>R. muscosa</i> a	GLLSSFKGVAKGVAKDLAGKLLLEKLEKCKITGC
592	<i>R. muscosa</i> b	GIMDSVKGVAKNLA****AKLLEKLEKCKITGC
593	<i>R. pretiosa</i> a	GILDSFKGVAKGVAKDLAGKLLDKLKCKITGC
594	<i>R. pretiosa</i> b	GILDTFKGVAKGVAKDLAVHMLENLKCKMTGC
595	<i>R. pretiosa</i> c	GILDSFKDVAKGVA****THLLNMAKCKMTGC
596	<i>R. pretiosa</i> d	GILSSIKGVAKGVAKNVAAQLLDTLKCKITGC
597	<i>R. pretiosa</i> e	GIMNTVKDVATGVA****THLLNMVKCKITGC
598	<i>R. pretiosa</i> f	GILDTFKGVAKGVAKDLAVHMLEKLEKCKMTGC
599	<i>R. pretiosa</i> g	GILSSFKDVAKGVAKNVAAQLLDKLKCKITGC
600	<i>R. pretiosa</i> h	GILDTVKGVAKDVA****AHLNLMVKCKITGC

601

602

603 Supplementary Fig. 2. Primary structures of 20 ranatuerin-2 peptides isolated from 7 *Rana*

604 species from the New World. In order to maximize structural similarity, amino acid gaps

605 denoted by * have been introduced into some sequences.

606

607

608

609

610

611

612